Am J Cancer Res 2026;16(6):2377-2388
www.ajcr.us /ISSN:2156-6976/ajcr0170905

Original Article

DDOST mediates cervical cancer cell malignant progression by interacting with SMARCA4

Biqing Zhu[1*], Yizhi Ge[1*], Yuxuan Wen[2*], Yinan Wu[3], Jinjie Yao[4], Jing Luo[2], Jing Wu[1], Dongfang Dai[1,5,6]

[1]Department of Radiation Oncology, The Affiliated Cancer Hospital of Nanjing Medical University, Jiangsu Cancer Hospital, Jiangsu Institute of Cancer Research, Nanjing 210000, Jiangsu, P. R. China; [2]Department of Cardiothoracic Surgery, Jinling Hospital, Affiliated Hospital of Medical School, Nanjing University, Nanjing 210000, Jiangsu, P. R. China; [3]Department of Pathology, The Affiliated Cancer Hospital of Nanjing Medical University, Jiangsu Cancer Hospital, Jiangsu Institute of Cancer Research, Nanjing 210000, Jiangsu, P. R. China; [4]School of Pharmacy, Nanjing University of Chinese Medicine, Nanjing 210000, Jiangsu, P. R. China; [5]Institute of Oncology, Affiliated Hospital of Jiangsu University, Zhenjiang 212000, Jiangsu, P. R. China; [6]Collaborative Innovation Center for Cancer Medicine, Nanjing Medical University, Nanjing 210000, Jiangsu, P. R. China. [*]Equal contributors.

Received December 20, 2025; Accepted June 2, 2026; Epub June 15, 2026; Published June 30, 2026

Abstract: DDOST is generally recognized as a regulator of glycosylation homeostasis and its deficiency can cause congenital glycosylation disorders. However, its role in tumors has not yet been elucidated. This study aimed to explore the functional role of DDOST and its related mechanisms in cervical cancer (CC). The clinical correlation of DDOST was analyzed using The Cancer Genome Atlas (TCGA) database and verified by immunohistochemistry slides of clinical samples. Cell growth, proliferation, apoptosis, migration, and invasion were evaluated. Co-immunoprecipitation (co-IP) and liquid chromatography with tandem mass spectrometry (LC-MS) were used to identify interacting proteins. The functions of the interacting proteins were further confirmed using genetic rescue experiments. A subcutaneous xenograft model was used to investigate tumorigenesis. Based on the TCGA data and our collected clinical samples, we found that DDOST was associated with a more aggressive pathological phenotype. DDOST also promoted several malignant phenotypes in CC cells. Co-IP coupled with LC-MS identified the interacting protein SMARCA4, and western blotting confirmed a positive interaction between these two proteins. Similar to in vivo tumorigenesis, cell growth and migration were markedly rescued by SMARCA4 overexpression after DDOST knockdown, as was tumorigenesis *in vivo*. This study showed that DDOST promoted tumorigenesis in CC and was identified it as a possible novel biomarker or therapeutic target in CC. The interaction between DDOST and SMARCA4 is a potential mechanism that requires further investigation.

Keywords: Cervical cancer, DDOST, malignant progression, SMARCA4, biomarker

Introduction

Cervical cancer (CC) is one of the most common malignancies and causes most of cancer-related deaths in women worldwide [1]. Despite the widespread use of early screening programs and multiple therapeutic methods, patients with advanced CC have a worse prognosis than those with early-stage CC. Once distant metastasis occurs, cure is rarely achieved [2] and the 5-year overall survival rate drops dramatically from 80% in stage I to less than 20% in stage IV [3]. Considering the high morbidity of CC worldwide, particularly in developing countries, further identification of metastatic biomarkers and identification of the molecular mechanisms involved are required.

DDOST encodes AGER1 protein, a subunit of the oligosaccharide transferase complex, which is involved in the endocytosis of advanced glycation end products (AGEs). Impaired DDOST expression usually causes AGEs to accumulate, resulting in pathogenesis of hyperglycemia and aging [4, 5]. However, most of the albeit limited studies have reported a correlation between DDOST and non-neoplastic diseases [6]. The potential role of DDOST in tumorigenesis, especially CC, is still poorly understood. DDOST is a conserved subunit of the oligosaccharyl trans-

https://doi.org/10.62347/JJQH4316

ferase complex in the endoplasmic reticulum and plays an essential role in N-linked glycosylation, protein maturation, and cellular proteostasis. Because proper glycosylation and protein quality control are required for the folding, stability, and trafficking of many membrane and secreted proteins, dysregulation of DDOST may have consequences beyond metabolic or non-neoplastic disorders [7]. In cancer, these homeostatic mechanisms can be co-opted to help tumor cells tolerate endoplasmic reticulum stress, sustain the processing of growth- and survival-related proteins, and adapt to the high biosynthetic demands of malignant progression. Therefore, although the role of DDOST in cervical cancer remains poorly understood, its known cellular functions provide a biological basis for hypothesizing that it may contribute to cervical cancer development and aggressiveness.

The aim of this study was to investigate the biological effects of DDOST on the malignant phenotype of CC. Co-immunoprecipitation (co-IP) and liquid chromatography-tandem mass spectrometry (LC-MS) were used to further explore the mechanism.

Materials and methods

Gene expression database and tumor samples

The clinical features of CC patients and the mRNA expression levels of DDOST were downloaded from The Cancer Genome Atlas (TCGA, https://cancergenome.nih.gov/). Fifty-one CC specimens were collected from the Affiliated Hospital of Jiangsu University. This study was approved by the Biomedical Research Ethics Committee of the Affiliated Hospital of Jiangsu University (Approval No. AF-SOP026-01), and all patients who met the inclusion criteria signed an informed consent. Detailed clinicopathological characteristics of these patients, including FIGO stage, histological grade, and lymph node status, were summarized in Table S4.

Cell culture

Human cervical cancer HeLa and SiHa cells were purchased from the Chinese Type Culture Collection Center and cultured in Dulbecco's Modified Eagle medium (DMEM, Gibco, Thermo) containing 10% fetal bovine serum (FBS, Gibco) and in a humidified incubator at 37°C with 5% CO_2. Cells in the logarithmic growth phase were trypsinized, passaged or used for subsequent experiments.

Immunohistochemistry (IHC)

The expression of DDOST in tumor tissues and adjacent tissues was analyzed by immunohistochemistry (IHC). Briefly, fresh tissues were fixed, deparaffinized, and rehydrated. After antigen repair, enzyme inactivation and blocking, the cells were incubated with 1:100 anti-DDOST antibody at 4°C overnight. After incubation with secondary antibodies for 50 min, the cells were stained with DAB and then the nuclei were re-stained. IHC scores of dehydrated and sealed tumor sections were assessed independently by two pathologists. The percentage of positive cells was scored as follows: 0 (< 10%), 1 (10-25%), 2 (26-50%), 3 (51-75%), 4 (> 75%). Staining intensity was scored as 0 for no staining, 1 for light brown, 2 for brown, and 3 for dark brown. The IHC score for DDOST is the product of the positive value and intensity. Scores < 8 were defined as low expression and scores ≥ 8 as high expression.

Construction of plasmid, lentiviral vector, and cell infection

A lentiviral vector (LV) with a short hairpin RNA (shRNA) sequence of DDOST (shDDOST) or control (shCtrl) was synthesized and then constructed with GV115 (hU6-MCS-CMV-EGFP). Overexpression of LV DDOST, SMARCA4, and CTNNB1 was achieved using GV491 (Ubi-3FLAG (Sigma)-MCS-SV40-puromycin), CV224 (Ubi-MCS-SV40-Cherry-IRES-puromycin), and GV661 (CMV-MCS-3FLAG-EF1-mCherry-T2A-puromycin), respectively. An empty vector was used as the negative control (NC). The recombinant lentiviruses were harvested from 293T cells and purified. Co-infection of knockdown and overexpression constructed LVs was performed using a combination of polybrene (50 μg/ml). The volume was calculated using a multiplicity of infection (MOI) of 20. The fluorescence intensity was determined 72 h after infection. Stable cell lines were filtered using puromycin (3 μg/ml). Transfection efficiency was validated using fluorescence (green or red), qRT-PCR, and western blotting. Primer sequences used are listed in Table S1.

Quantitative reverse transcription PCR (RT-qPCR)

Total cellular RNA was extracted using TRIzol (Invitrogen) and transcribed to cDNA using the Promega M-MLV kit. RT-qPCR was performed with Takara SYBR Master Mix and MX3000p system (Agilent). Relative mRNA expression was calculated using the $2^{-\Delta\Delta CT}$ method and GAPDH was used as a standard. Primer sequences are listed in Table S2.

Cell growth, proliferation and colony formation

Three days after transfection, cell growth, proliferation and colony formation were detected by fluorescence assay, Cell Counting Kit-8 (CCK-8) kit (Dojindo) and colony formation assay, respectively. Briefly, 2000 cells per well were seeded in 96 Wells for cell growth and proliferation assays. The number of cells showing green fluorescence was measured daily using a Celigo Image Cytometer (Nexcelom) for 3 to 5 consecutive days. One hundred cells were seeded in 6 well-plates for the colony formation assay. Colony counts were performed using ImageJ after 9 d.

Cell apoptosis

An Annexin V-APC/PI apoptosis kit (eBioscience) was applied to detect apoptosis. The cells were collected and washed thrice with cold phosphate-buffered saline (PBS). Staining was performed according to the manufacturer's protocol and the percentage of apoptotic cells was evaluated using a Flow Cytometer (BD Biosciences).

Cell migration and invasion

Migration and invasion abilities were assessed as described previously [8]. Transwell and Matrigel kits (Corning) were used according to the manufacturer's guidelines. Briefly, 8×10^4 cells were seeded in the upper chamber of 24-well serum-free medium. Complete medium was then added to the lower chamber. The inserts in the Transwell kit had an 8 μm pore size and were coated with Matrigel. After 24 h of culture, migrating and invading cells were fixed, stained, and counted at 5 random fields using an Olympus microscope.

Western blot

Cells were harvested and incubated with pre-cooled 2×Lysis buffer for 10 to 15 min on ice. Lysates were then crushed by sonication and total proteins were extracted by centrifugation. Protein concentrations were quantified with a bicinchoninic acid (BCA) Protein assay Kit (Beyotime). Protein samples were separated by 10% sodium dodecyl sulfate-polyacrylamide gel electrophoresis (SDS-PAGE), transferred to polyvinylidene difluoride (PVDF) membranes (Millipore), blocked with Tris-buffered saline containing Tween 20 (TBST) and 5% skim milk, and incubated with primary and secondary antibodies. Antibodies included anti-DDOST (1:200, Abcam), anti-SMARCA4 (1:10,000, Abcam), anti-CTNNB1 (1:1,000, Abcam), anti-FLAG (1:2,000, Sigma), and anti-GAPDH (1:2,000, Abcam). Secondary antibodies (1:10000) were purchased from Cell Signaling Technology (CST). Immunoreactive bands were detected using the enhanced chemiluminescence (ECL)-PLUS kit (Thermo Fisher Scientific).

Co-immunoprecipitation (co-IP)

SiHa cells stably overexpressing DDOST were constructed, and cells were infected with FLAG-tagged lentivirus particles in the presence of 3 μg/mL puromycin. Western blot was used to verify the transfection effect. Total protein was extracted and incubated with FLAG beads (Sigma-Aldrich) overnight. After washing, the samples were exchanged with 3×Flag peptide, and precipitated proteins were screened by SDS-PAGE or detected by western blotting.

LC-MS analysis

Proteomic analyses were conducted using shotgun analysis and liquid chromatography with tandem mass spectrometry (LC-MS). Briefly, the SDS-PAGE gel was stained with Coomassie Brilliant Blue, digested with trypsin, desalinated, and separated using an Easy nLC system. Finally, the samples were analyzed using a Q-Exactive Plus mass spectrometer. Proteome Discoverer 2.1 (Thermo Fisher Scientific) and MASCOT 2.2 (Matrix Science, London, UK) were used to analyze the raw data.

GO and KEGG analysis

Annotation of proteins specifically identified in the overexpression group was performed using Gene Ontology (GO) and Kyoto Encyclopedia of Genes and Genomes (KEGG). GO functional annotation was performed using National

Table 1. The relationship between pathological information and DDOST mRNA expression in cervical cancer patients from TCGA

Pathological Grading or Stage	mRNA Level. No.		Total No.	*P* value
	Low (%)	High (%)		
T				
T1	73 (52.1)	67 (47.9)	140	0.63
T2	36 (50.7)	35 (49.3)	71	
T3/4	14 (46.7)	16 (53.3)	30	
N				
N0	67 (50.4)	66 (49.6)	133	0.553
N1	33 (55)	27 (45)	60	
M				
M0	53 (45.9)	63 (54.3)	116	0.73
M1	4 (40)	6 (60)	10	
Grade				
1-2	88 (57.5)	65 (42.5)	153	0.008
3-4	49 (41.2)	70 (58.8)	119	
Stage				
I	78 (48.1)	84 (51.9)	162	0.579
II	38 (55.1)	31 (44.9)	69	
III/IV	33 (50)	33 (50)	66	

Abbreviations: TCGA, The Cancer Genome Atlas; mRNA, messenger RNA. In the TNM staging system, T indicates primary tumor extent, N indicates regional lymph node involvement, and M indicates distant metastasis.

Center for Biotechnology Information (NCBI) BLAST (ncbi-blast-2.3.0) and Blast2GO methods, coupled with additional annotation from InterProScan and the European Bioinformatics Institute (EBI) databases. KEEG pathway analysis was completed with KOALA (KEGG Orthology and Links Annotation (KOALA)) software by matching the KEGG Genes database. A Venn diagram was constructed using the bioinformatics website (http://bioinformatics.psb.ugent.be/webtools/Venn/).

Animal experiment

The stable transfected SiHa cells (5×10^6) were inoculated subcutaneously into the right armpit of 5-week-old female BALB/c nude mice. Subcutaneous tumors were measured three times per week using calipers and tumor volume was calculated as tumor volume = (length × width^2)/2. The largest tumor diameter does not exceed 2.0 cm and mice with tumor volume ≥ 1000 mm^3 were sacrificed. The mice were euthanized by carbon dioxide (CO_2) inhalation followed by cervical dislocation. All animal experiments were reviewed and approved by the Institutional Animal Care and Use Committee of Shanghai GeneChem Co., Ltd. (Approval No. NYDLS-2018-116) and were performed in accordance with institutional guidelines for the care and use of animals.

Statistical analysis

All experiments were independently replicated three times and analyzed using GraphPad Prism 7.0 and Photoshop. All data were presented as mean ± standard deviation (SD). Survival analysis was performed using the Kaplan-Meier method and the log-rank test. Spearman's correlation analysis was conducted using the SPSS software (version 19.0). For experiments involving repeated measurements over time, including cell growth curves and xenograft tumor growth curves, repeated-measures ANOVA was used. The student's t-test (two-tailed) was used to identify differences between two groups. Quantitative variables with non-normal distributions were compared using the Mann-Whitney U test. The count data were presented as numbers and percentages. Intergroup comparisons of count data were carried out using the Chi-square test. $P < 0.05$ was considered statistically significant.

Results

DDOST upregulation was associated with advanced tumor grade and worse survival in TCGA data

To identify the role of DDOST in patients with CC, we analyzed the clinical correlation of DDOST. A total of 303 patients with RNA sequencing (RNA-seq) and pathological information were identified in TCGA database. As indicated in **Table 1**, the mRNA levels of DDOST were significantly differentially expressed in patients with CC of different pathological grades (P=0.008). Higher expression of DDOST was associated with an advanced pathological grade ($P < 0.05$), despite low Spearman's correlation coefficients (Table S3). IHC of our clinical patient specimens confirmed the higher

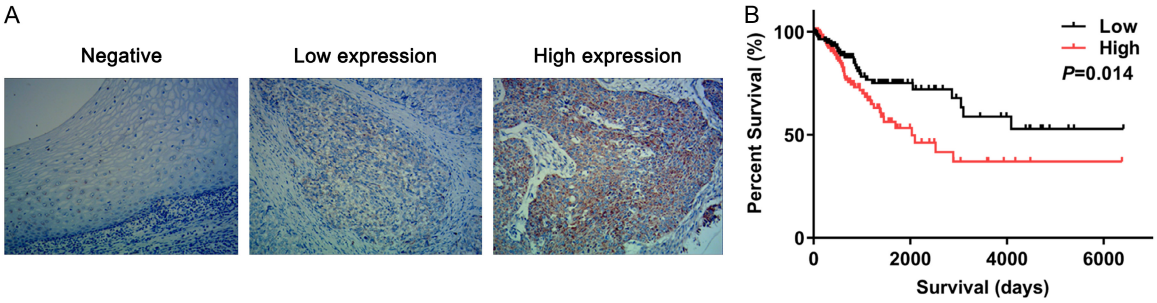

Figure 1. DDOST upregulation was associated with advanced tumor grade and worse survival in TCGA data and our hospital database. (A) Representative immunohistochemistry (IHC) images of negative control tissue (left) and tumor tissues with low (middle) and high (right) DDOST expression. Magnification, ×200. (B) Kaplan-Meier overall survival curves of patients with cervical cancer in The Cancer Genome Atlas (TCGA) cohort stratified by DDOST expression level. Survival differences were analyzed using the log-rank test. The *P* value in (B) was calculated using the log-rank test.

protein expression of DDOST in tumors than in normal tissues (**Figure 1A**) and a positive correlation between DDOST and pathological grade (Table S4).

Kaplan-Meier survival analysis indicated that patients with higher DDOST mRNA expression had markedly worse overall survival (OS) than those with lower expression in TCGA (P=0.014, **Figure 1B**). These results elucidate the potential adverse impact of DDOST on the malignant progression of CC as well as its poor prognosis.

DDOST promoted the malignant phenotypes of CC cells

The mRNA and protein expression levels of DDOST in HeLa and SiHa cells are shown in **Figure 2A**. To explore the functional effect of DDOST on CC cells, we transfected CaSKi and SiHa cells with lentivirus particles containing an RNA interference (RNAi) sequence of DDOST. Cell status and infection efficiency were observed using green fluorescent protein (GFP) fluorescence three days after infection (**Figure 2B**). RT-qPCR and western blotting confirmed that DDOST expression was successfully knocked down (**Figure 2C**). The overexpression efficiency of DDOST in CASKI and SiHa cells at the protein level was represented by Flag (**Figure 2D**). DDOST inhibition significantly reduced cell growth (**Figure 2E**). In addition, inhibition of DDOST reduced cell viability and colony counts in CC cells compared with those in the control group (all $P < 0.05$, **Figure 2F**). Migration and invasion abilities were significantly attenuated after DDOST inhibition (all P values < 0.05, **Figure 2G**, **2H**). These results showed the opposite trend with the overexpression of DDOST (**Figure 2E-H**).

Flow cytometry was used to determine the apoptosis rate of CC cells with DDOST silencing, followed by Annexin V-APC/PI staining. The percentage of apoptotic cells was significantly higher in the treatment group than in the control group ($P < 0.05$, **Figure 3A**). These results demonstrated that DDOST promoted the malignant phenotypes of CC cells, which were weakened after DDOST knockdown.

SMARCA4 interacted and positively correlated with DDOST in CC cells

Although DDOST expression was initially assessed in cervical cancer cell lines, SiHa cells were selected for the in-depth mechanistic studies because DDOST overexpression/knockdown in SiHa cells showed stable and reproducible modulation efficiency with clear phenotypic changes, making them more suitable for the establishment of stable cell models for co-IP/LC-MS, rescue experiments, and xenograft assays. For consistency, the subsequent mechanistic validation was therefore mainly performed in SiHa cells. To explore the binding of interacting proteins to DDOST, co-IP coupled with LC-MS was performed in stably transfected DDOST overexpression SiHa cells. The expression level of DDOST was detected via Flag by western blotting (**Figure 3B**). The SDS-PAGE gel of the DDOST immunoprecipitates was digested and analyzed by LC-MS. In total, 1,229 and 1,174 protein groups were identified in the control and overexpression

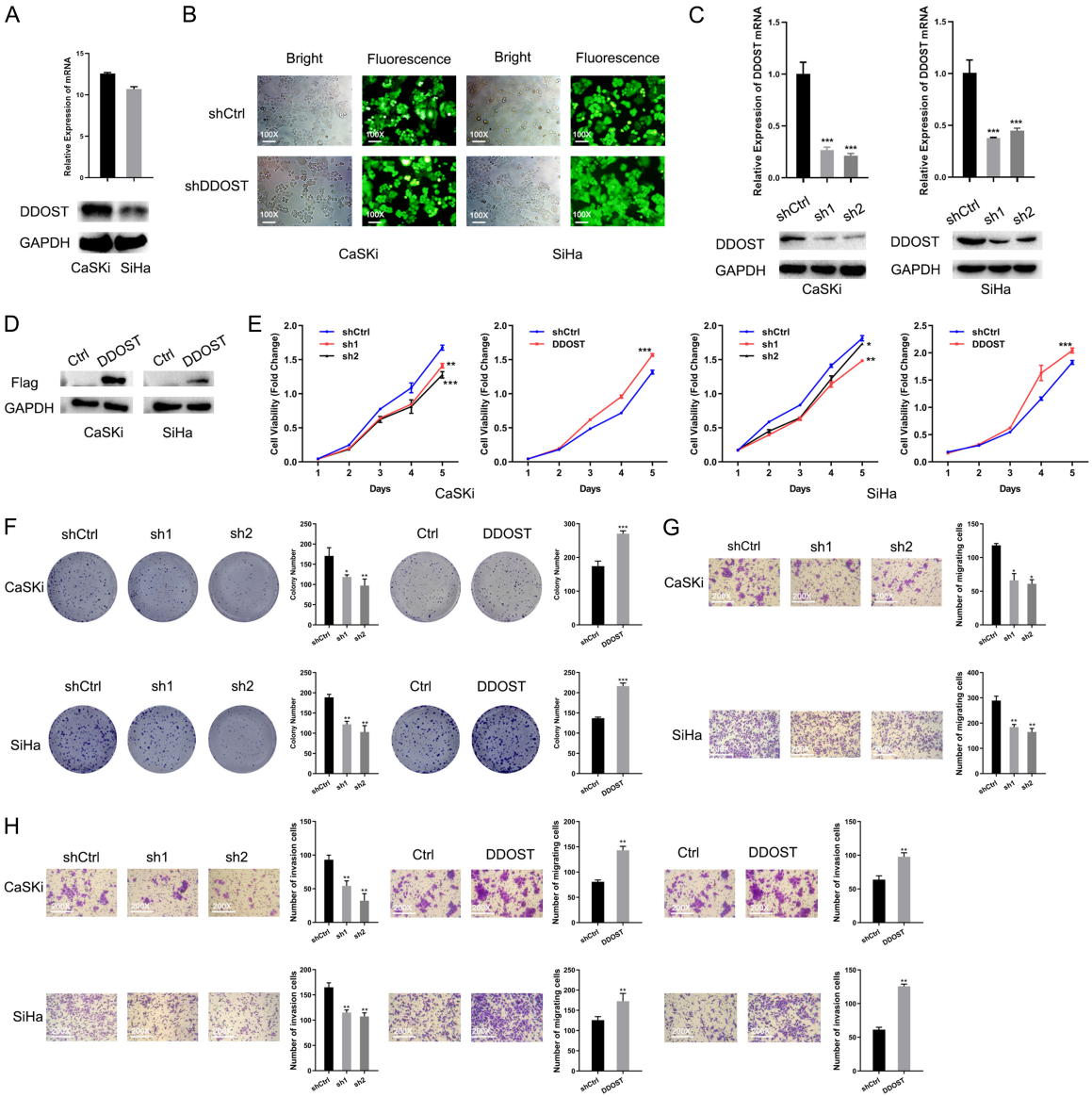

Figure 2. DDOST promoted the malignant phenotypes of CC cells. (A) mRNA (left) and protein (right) expression levels of DDOST normalized to GAPDH in CaSKi and SiHa cells, as detected by quantitative reverse transcription polymerase chain reaction (qRT-PCR) and western blot in CASKI and SiHa cells. Representative fluorescent images of cells (magnification 100×) (B) and knockdown efficiency (C) of DDOST in CASKI and SiHa cells in mRNA (left), and protein (right) expression level after transfection with short hairpin RNA (shRNA) for three days. Overexpression efficiency of DDOST in CASKI and SiHa cells in protein level represented by FLAG-tag (D). Cell Counting Kit-8 (CCK-8) assay (E), colony formation (magnification 1×) (F), transwell (magnification 200×) (G), and invasion (magnification 200×) (H) experiment of CASKI (left) and SiHa (right) cells. Data are presented as mean ± SD from three independent experiments. Statistical significance is indicated as follows: *P < 0.05, **P < 0.01, ***P < 0.001; ns, not significant; comparisons were made with the corresponding control group.

(OE) samples, respectively (**Figure 3C**). A total of 333 proteins were exclusively identified in the DDOST-overexpression group and were enriched by GO and KEGG analyses (**Figure 3D**). Among the proteins specifically identified in the DDOST-overexpression group, SMARCA4 and CTNNB1 were prioritized for further validation because both are biologically relevant to malignant phenotypes observed in this study, including proliferation, apoptosis, migration, and invasion. We therefore examined whether DDOST interacted with these candidate proteins by immunoprecipitation (IP) assay, which confirmed interactions of DDOST with both

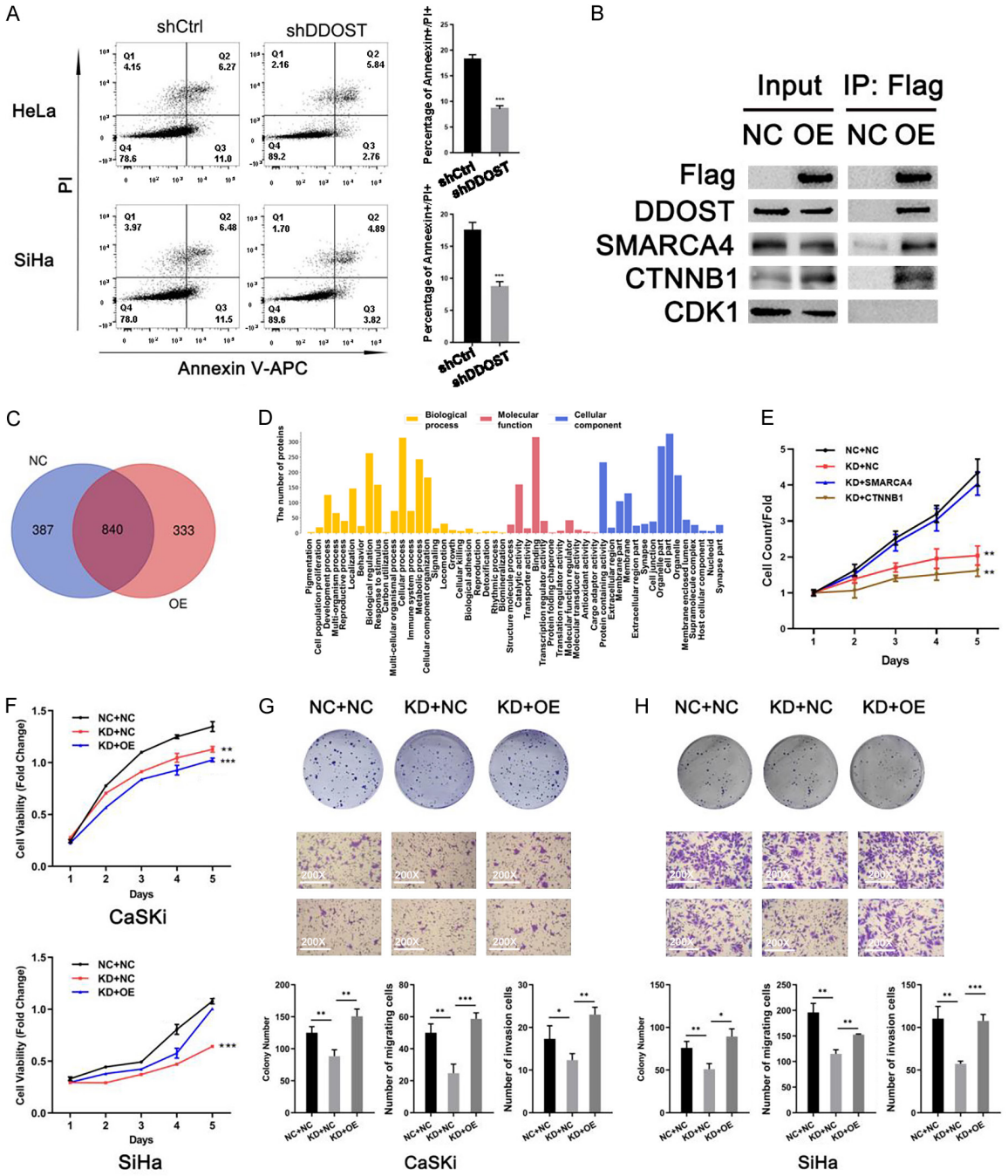

Figure 3. SMARCA4 interacted and exerted a synergized role with DDOST in CC cells. (A) Cell apoptosis was detected by flow cytometric analysis after transfection and incubation for 3 and 2 days in HeLa (top) and SiHa (bottom) cells, respectively. (B) The results of co-immunoprecipitation (co-IP) and western blot experiments confirmed the interaction between DDOST and identified proteins. (C) Venn diagram of total proteins identified by liquid chromatography-tandem mass spectrometry (LC-MS) analysis in NC and OE group of SiHa cells. NC, negative control; OE, DDOST overexpression. (D) Gene Ontology (GO) analysis of exclusively expressed in DDOST OE group. (E) Cell viability of SMARCA4 and CTNNB1. Growth in CaSKi and SiHa (F), and the ability of colony formation (top, magnification 1×) and migratory (bottom, magnification 200×) in stably-transfected (G) CaSKi and (H) SiHa cells. NC, negative control; KD, DDOST knockdown; OE, SMARCA4 overexpression. Data are presented as mean ± SD from three independent experiments. Statistical significance is indicated as follows: *P < 0.05, **P < 0.01, ***P < 0.001; ns, not significant; Statistical significance refers to the comparisons indicated in the figure.

SMARCA4 and CTNNB1 (**Figure 3B**). Subsequent rescue experiments showed that SMARCA4, but not CTNNB1, substantially restored the malignant phenotypes suppressed by DDOST

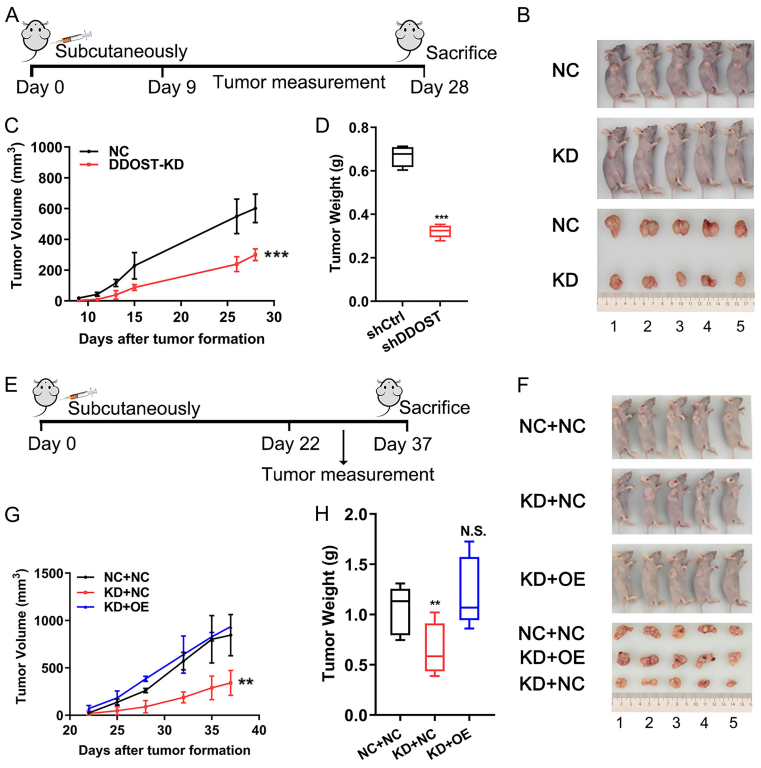

Figure 4. SMARCA4 overexpression reversed tumor growth reduced by DDOST knockdown in a xenograft mouse model. Scheme of animal analysis (A), images of the xenograft model (B), tumor growth (C), and weight (D) of tumor-bearing nude mice subcutaneously injected with shDDOST and NC-transfected SiHa cells. Scheme of animal analysis (E), images of the xenograft model (F), tumor growth (G), and weight (H) of tumor-bearing nude mice subcutaneously injected with shDDOST and SMARCA4 co-transfected SiHa cells. Representative xenograft images were retaken with a ruler as a size reference. Tumor growth was monitored three times weekly, and mice were euthanized before any tumor exceeded 2.0 cm in the largest diameter. Data are presented as mean ± SD. Statistical significance is indicated as follows: *P < 0.05, **P < 0.01, ***P < 0.001; ns, not significant; comparisons were made between the indicated groups.

knockdown (**Figure 3E**), and SMARCA4 was therefore selected for further mechanistic validation. Subsequently, we examined the reversal function of the screened interacting genes in SiHa cell growth and migration.

Overexpression of SMARCA4 rescued the malignant phenotype after DDOST knockdown in CC cells

After co-transfecting lentivirus particles with green or red fluorescence and validating by qRT-PCR (Figure S1A, S1B), cell growth was slowed down after knockdown of DDOST, and was largely recovered by SMARCA4 overexpression, but not by CTNNB1 (**Figure 3E**). Therefore, SMARCA4 was selected to further validate the functional recovery experiments. The proliferation viability of CaKSi and SiHa cells with DDOST knockdown significantly decreased ($P < 0.05$), which was consistent with our expectations. Viability increased nearly to the original level, followed by overexpression of SMARCA4 ($P < 0.05$, **Figure 3F**), and migratory and colony formation abilities also increased close to the original level (**Figure 3G**, **3H**). The results showed that the overexpression of SMARCA4 rescued the proliferation and migration phenotype of the DDOST knockdown group.

Animal studies confirmed the biological function of DDOST and SMARCA4

To confirm the relationship between DDOST and SMARCA4 *in vivo*, a subcutaneous xenograft nude mouse model was used. After 28 days of observation, the tumor volume and weight were obviously reduced after DDOST knockdown (**Figure 4A-D**). The inhibitory effect of the DDOST knockdown was rescued by SMARCA4 overexpression (**Figure 4E-H**), similar to the phenotypes observed above. Furthermore, the impacts of DDOST knockdown on the proliferation marker (Ki-67) and apoptosis marker (cleaved caspase-3) could be partially reversed by overexpression of SMARCA4 (Figure S2). These findings elucidate the synergistic functions of DDOST and SMARCA4 during CC progression. Downregulation of tumorigenic ability by shDDOST was reversed by SMARCA4.

Discussion

The biological function of DDOST in CC was investigated for the first time in the present study. We found that DDOST promoted tumor growth, proliferation, migration, and invasion, while inhibiting apoptosis. These malignant

phenotypes were inhibited by DDOST knockdown, both *in vitro* and *in vivo*. Co-IP coupled with LC-MS identified the interacting protein SMARCA4, which was confirmed by IP and western blotting. Moreover, the inhibitory phenotype of shDDOST was significantly rescued by SMARCA4 overexpression. These results suggest that DDOST expression gradually increases with disease progression. Specific pathways and their interactions require further evaluation.

DDOST is a polypeptide subunit identified in the pancreatic microsomal membranes, and its genomic sequence was first reported by Momoi in 1997 [9]. The encoded conserved protein, AGER1, participates in AGE circulation and clearance as a related receptor [10]. Alternatively, AGER1 glycosylates the N-terminus of key kidney proteins to maintain kidney health and function [11]. Contradictory conclusions were derived from two clinical studies that discussed the involvement of AGER1 in diabetic nephropathy [12, 13]. Thereafter, the role of DDOST in disorders of glycosylation, diabetes and nonalcoholic steatohepatitis is unknown [4, 5, 14, 15]. SMARCA4 encodes a homonymous protein necessary for the transcription of certain genes. It acts as a tumor suppressor and is frequently inactivated in cancers with undruggable traits [16]. The spectrum of SMARCA4 alteration in patients with solid tumors has recently been elucidated [17]. Multiple tumors have been associated with the deficiency or mutation of SMARCA4 [18-20].

Emerging evidence has been used to determine the relationship between DDOST and oropharyngeal, bladder, colon, and esophageal cancer [21-24]. However, the specific phenotypes and mechanisms underlying CC remain to be elucidated. Our results illustrate the effect of DDOST on the malignant phenotype of CC cells. DDOST expression was positively associated with higher pathological grade and negatively associated with prognosis. DDOST knockdown inhibited tumor growth, proliferation, migration, and invasion and promoted apoptosis. Interestingly, co-IP followed by LC-MS revealed an interaction between the DDOST and SMARCA4 proteins. After overexpression of SMARCA4, tumor growth and migration were observed. Subsequent *in vivo* experiments validated the synergistic efficiency of DDOST and SMARCA4. More importantly, TCGA database and our clinical samples confirmed the advanced stage and survival results of DDOST.

Notably, in the TCGA cohort, DDOST expression was significantly associated with pathological grade but not with T, N, M, or FIGO stage. We believe this finding suggests that DDOST may be more closely related to the intrinsic aggressiveness and dedifferentiation of cervical cancer cells than to the anatomical extent of tumor spread. Pathological grade reflects tumor cell differentiation status, whereas TNM/FIGO stage mainly reflects tumor burden and dissemination. In line with this interpretation, our in vitro and in vivo data showed that DDOST enhanced proliferation, migration, invasion, and survival-related phenotypes, supporting a role in malignant biological behavior. Nevertheless, because the advanced-stage subgroups in TCGA were relatively limited, especially the metastatic subgroup, larger cohorts will be needed to further clarify whether DDOST is also associated with nodal or distant spread.

Interestingly, although both SMARCA4 and CTNNB1 were identified as DDOST-interacting candidates, only SMARCA4 overexpression significantly rescued the phenotypic defects caused by DDOST knockdown. This finding suggests that, in our model, SMARCA4 may represent a more functionally critical downstream effector of DDOST than CTNNB1 alone. Notably, this does not necessarily indicate that the DDOST-SMARCA4 axis is fully independent of canonical Wnt/β-catenin signaling. Since canonical Wnt activity was not directly evaluated in the present study, CTNNB1 overexpression may simply have been insufficient to restore the full transcriptional program disrupted by DDOST depletion. Given the known role of SMARCA4/BRG1 in chromatin remodeling and β-catenin-associated transcription, it is possible that SMARCA4 functions as a permissive or more proximal regulatory node in this context. Future studies should further examine nuclear β-catenin activity, TCF/LEF-dependent transcription, and classical Wnt target genes to clarify the relationship between DDOST-SMARCA4 signaling and the canonical Wnt pathway [25-28].

It should be noted that the mechanistic interpretation of the DDOST-SMARCA4 association

requires caution. Although co-IP/LC-MS and rescue experiments supported a functional link between DDOST and SMARCA4, the spatial and biochemical basis of this association remains unclear. Given that DDOST is primarily considered an endoplasmic reticulum-associated protein, whereas SMARCA4 is mainly a nuclear chromatin remodeler, the co-IP signal observed in whole-cell lysates may reflect a transient or indirect association within a larger protein complex rather than a stable direct interaction in a single subcellular compartment. We therefore propose a working model in which DDOST promotes cervical cancer progression partly through a DDOST-SMARCA4 functional axis, potentially by influencing SMARCA4 protein stability and/or transcriptional output. However, whether DDOST affects the subcellular localization, half-life, chromatin occupancy, or transcriptional regulatory activity of SMARCA4 requires further investigation. Future studies using subcellular fractionation, immunofluorescence, reciprocal endogenous co-IP, proximity ligation assays, protein stability assays, and chromatin/transcriptome profiling will be needed to clarify this mechanism.

Our study is the first to demonstrate that DDOST could be a biomarker for tumor progression and a potential therapeutic target. The interaction between DDOST and SMARCA4 may be a potential mechanism that requires further investigation. Collectively, our findings suggest that DDOST may serve as a potential biomarker associated with advanced disease and poor prognosis in cervical cancer, although these observations still require further validation in larger and more mechanistically detailed studies.

Limitations

This study has several limitations that should be acknowledged. First, although we identified the interaction between DDOST and SMARCA4 by co-immunoprecipitation/LC-MS and supported its functional relevance through rescue experiments, the mechanistic investigation remains at the level of protein interaction identification and phenotypic association. The precise downstream signaling pathways and molecular events through which DDOST cooperates with SMARCA4 to promote cervical cancer progression were not fully elucidated. Second, the in vivo evidence was derived from a subcutaneous xenograft model, which cannot fully recapitulate the native cervical tumor microenvironment or the complex metastatic process of cervical cancer. Third, the clinical validation cohort was obtained from a single center and included a relatively limited number of samples, which may restrict the generalizability of the findings. Therefore, larger multicenter studies, together with orthotopic or metastasis-relevant animal models and more in-depth mechanistic investigations, are warranted to further validate and extend our conclusions.

Conclusion

In conclusion, we revealed a promotional effect of DDOST on CC. The interacting protein, SMARCA4, which exerts a synergistic effect on CC cells, was also identified. DDOST may be a possible screening biomarker and druggable target for CC diagnosis and treatment.

Acknowledgements

This study was supported by Postdoctoral Funding of Jiangsu Cancer Hospital (No. SZL202016), Postdoctoral Science Foundation of Jiangsu Province (No. 200730000107 and No. 2021Z282), National Natural Science Foundation for Youth of China (No. 82202932 and No. 82103552), National Natural Science Foundation of China (No. 82273325), and Natural Science Foundation for Youth of Jiangsu Province (No. BK20220735).

The patients provided their written informed consent to participate in this study.

Disclosure of conflict of interest

None.

Address correspondence to: Dongfang Dai and Jing Wu, Department of Radiation Oncology, The Affiliated Cancer Hospital of Nanjing Medical University, Jiangsu Cancer Hospital, Jiangsu Institute of Cancer Research, 42 Baiziting Road, Nanjing 210000, Jiangsu, P. R. China. E-mail: ddfszl@njmu.edu.cn (DFD); wmz18@njmu.edu.cn (JW); Jing Luo, Department of Cardiothoracic Surgery, Jinling Hospital, Medical School of Nanjing University, 305 East Zhongshan Road, Nanjing 210000, Jiangsu, P. R. China. E-mail: luojing@jssexzlfzswxj.wecom.work

References

[1] Siegel RL, Kratzer TB, Giaquinto AN, Sung H and Jemal A. Cancer statistics, 2025. CA Cancer J Clin 2025; 75: 10-45.

[2] Zhang H, Luo X, Jiang J, Zhang C, Li L, Chen Y, Zeng Y, Zhou F, Liu Y, Liu Y and Li Y. The clinical application value of dynamic monitoring of HPV ctDNA in concurrent chemoradiotherapy for locally advanced cervical cancer. NPJ Precis Oncol 2026; 10: 150.

[3] Grigsby PW, Massad LS, Mutch DG, Powell MA, Thaker PH, McCourt C, Hagemann A, Fuh K, Kuroki L, Schwarz JK, Markovina S, Lin AL, Dehdashti F and Siegel BA. FIGO 2018 staging criteria for cervical cancer: Impact on stage migration and survival. Gynecol Oncol 2020; 157: 639-643.

[4] Dehnad A, Fan W, Jiang JX, Fish SR, Li Y, Das S, Mozes G, Wong KA, Olson KA, Charville GW, Ali M and Török NJ. AGER1 downregulation associates with fibrosis in nonalcoholic steatohepatitis and type 2 diabetes. J Clin Invest 2020; 130: 4320-4330.

[5] Santos-Bezerra DP, Machado-Lima A, Monteiro MB, Admoni SN, Perez RV, Machado CG, Shimizu MH, Cavaleiro AM, ThiemeK, Queiroz MS, Machado UF, Giannella-Neto D, Passarelli M and Corrêa-Giannella ML. Dietary advanced glycated end-products and medicines influence the expression of SIRT1 and DDOST in peripheral mononuclear cells from long-term type 1 diabetes patients. Diab Vasc Dis Res 2018; 15: 81-89.

[6] Sun H and Xie C. Progress in research on DDOST dysregulation in related diseases. Glycoconj J 2025; 42: 125-135.

[7] Kas SM, Mundra PA, Smith DL and Marais R. Functional classification of DDOST variants of uncertain clinical significance in congenital disorders of glycosylation. Sci Rep 2023; 13: 17648.

[8] Wang W, Li X, Xu Y, Guo W, Yu H, Zhang L, Wang Y and Chen X. Acetylation-stabilized chloride intracellular channel 1 exerts a tumor-promoting effect on cervical cancer cells by activating NF-kappaB. Cell Oncol (Dordr) 2021; 44: 557-568.

[9] Yamagata T, Tsuru T, Momoi MY, Suwa K, Nozaki Y, Mukasa T, Ohashi H, Fukushima Y and Momoi T. Genome organization of human 48-kDa oligosaccharyltransferase (DDOST). Genomics 1997; 45: 535-540.

[10] Gong Y, Liu Z, Zhang Y, Zhang J, Zheng Y and Wu Z. AGER1 deficiency-triggered ferroptosis drives fibrosis progression in nonalcoholic steatohepatitis with type 2 diabetes mellitus. Cell Death Discov 2023; 9: 178.

[11] Yan K, Khoshnoodi J, Ruotsalainen V and Tryggvason K. N-linked glycosylation is critical for the plasma membrane localization of nephrin. J Am Soc Nephrol 2002; 13: 1385-1389.

[12] Hoverfelt A, Sallinen R, Söderlund JM, Forsblom C, Pettersson-Fernholm K, Parkkonen M, Groop PH and Wessman M; FinnDiane Study Group. DDOST, PRKCSH and LGALS3, which encode AGE-receptors 1, 2 and 3, respectively, are not associated with diabetic nephropathy in type 1 diabetes. Diabetologia 2010; 53: 1903-1907.

[13] He CJ, Koschinsky T, Buenting C and Vlassara H. Presence of diabetic complications in type 1 diabetic patients correlates with low expression of mononuclear cell AGE-receptor-1 and elevated serum AGE. Mol Med. 2001; 7: 159-168.

[14] Jones MA, Ng BG, Bhide S, Chin E, Rhodenizer D, He P, Losfeld ME, He M, Raymond K, Berry G, Freeze HH and Hegde MR. DDOST mutations identified by whole-exome sequencing are implicated in congenital disorders of glycosylation. Am J Hum Genet 2012; 90: 363-368.

[15] Uribarri J, Cai W, Ramdas M, Goodman S, Pyzik R, Chen X, Zhu L, Striker GE and Vlassara H. Restriction of advanced glycation end products improves insulin resistance in human type 2 diabetes: potential role of AGER1 and SIRT1. Diabetes Care 2011; 34: 1610-1616.

[16] Xue Y, Meehan B, Fu Z, Wang XQD, Fiset PO, Rieker R, Levins C, Kong T, Zhu X, Morin G, Skerritt L, Herpel E, Venneti S, Martinez D, Judkins AR, Jung S, Camilleri-Broet S, Gonzalez AV, Guiot MC, Lockwood WW, Spicer JD, Agaimy A, Pastor WA, Dostie J, Rak J, Foulkes WD and Huang S. SMARCA4 loss is synthetic lethal with CDK4/6 inhibition in non-small cell lung cancer. Nature communications 2019; 10: 557.

[17] Fernando TM, Piskol R, Bainer R, Sokol ES, Trabucco SE, Zhang Q, Trinh H, Maund S, Kschonsak M, Chaudhuri S, Modrusan Z, Januario T and Yauch RL. Functional characterization of SMARCA4 variants identified by targeted exome-sequencing of 131,668 cancer patients. Nat Commun 2020; 11: 5551.

[18] Stewart BD, Kaye F, Machuca T, Mehta HJ, Mohammed TL, Newsom KJ and Starostik P. SMARCA4-deficient thoracic sarcoma: a case report and review of literature. Int J Surg Pathol 2020; 28: 102-108.

[19] Schoenfeld AJ, Bandlamudi C, Lavery JA, Montecalvo J, Namakydoust A, Rizvi H, Egger J, Concepcion CP, Paul S, Arcila ME, Daneshbod Y, Chang J, Sauter JL, Beras A, Ladanyi M, Jacks T, Rudin CM, Taylor BS, Donoghue MTA, Heller G, Hellmann MD, Rekhtman N and Riely GJ. The genomic landscape of SMARCA4 alterations and associations with outcomes in pa-

tients with lung cancer. Clin Cancer Res 2020; 26: 5701-5708.
[20] Kolin DL, Quick CM, Dong F, Fletcher CDM, Stewart CJR, Soma A, Hornick JL, Nucci MR and Howitt BE. SMARCA4-deficient uterine sarcoma and undifferentiated endometrial carcinoma are distinct clinicopathologic entities. Am J Surg Pathol 2020; 44: 263-270.
[21] Shapanis A, Lai C, Smith S, Coltart G, Sommerlad M, Schofield J, Parkinson E, Skipp P and Healy E. Identification of proteins associated with development of metastasis from cutaneous squamous cell carcinomas (cSCCs) via proteomic analysis of primary cSCCs. Br J Dermatol 2021; 184: 709-721.
[22] Zhang Y, Fang L, Zang Y and Xu Z. Identification of core genes and key pathways via integrated analysis of gene expression and DNA methylation profiles in bladder cancer. Med Sci Monit 2018; 24: 3024-3033.
[23] Hu M, Fu X, Si Z, Li C, Sun J, Du X and Zhang H. Identification of differently expressed genes associated with prognosis and growth in colon adenocarcinoma based on integrated bioinformatics analysis. Front Genet 2019; 10: 1245.
[24] Donner I, Katainen R, Tanskanen T, Kaasinen E, Aavikko M, Ovaska K, Artama M, Pukkala E and Aaltonen LA. Candidate susceptibility variants for esophageal squamous cell carcinoma. Genes Chromosomes Cancer 2017; 56: 453-459.
[25] Barker N, Hurlstone A, Musisi H, Miles A, Bienz M and Clevers H. The chromatin remodelling factor Brg-1 interacts with beta-catenin to promote target gene activation. EMBO J 2001; 20: 4935-4943.
[26] Nakamura Y, de Paiva Alves E, Veenstra GJ and Hoppler S. Tissue- and stage-specific Wnt target gene expression is controlled subsequent to beta-catenin recruitment to cis-regulatory modules. Development 2016; 143: 1914-1925.
[27] Holik AZ, Young M, Krzystyniak J, Williams GT, Metzger D, Shorning BY and Clarke AR. Brg1 loss attenuates aberrant wnt-signalling and prevents wnt-dependent tumourigenesis in the murine small intestine. PLoS Genet 2014; 10: e1004453.
[28] Curtis CD and Griffin CT. The chromatin-remodeling enzymes BRG1 and CHD4 antagonistically regulate vascular Wnt signaling. Mol Cell Biol 2012; 32: 1312-1320.

Table S1. Primer sequence for shRNA and siRNAs synthesis information

Name		Primer Sequence (5' to 3')
shDDOST	Forward	CCGGCTCACATTCAAGACCGCTGATCTCGAGATCAGC GGTCTTGAATGTGAG
	Reverse	AATTCAAAAACTCACATTCAAGACCGCTGATCTCGAG ATCAGCGGTCTTGAATGTGAG
oeDDOST	Forward	CAGCTAGCGTTATTGAATTCATGGAGCCCAGCACCGC GGC
	Reverse	TTCCACAGGAATCAGAATTCTCAGTCGGACTTCTCCTT CTCCTTC
oeCTNNB1	Forward	GATCTATTTCCGGTGAATTCCGCCACCATGGCTACTCA AGCTGATTTG
	Reverse	TCCTTGTAGTCCATGGATCCCAGGTCAGTATCAAACCA GGCCAG
oeSMARCA4	Forward	AGGTCGACTCTAGAGGATCCCGCCACCATGTCCACTCC AGACCCACCCCTGGGC
	Reverse	CACACATTCCACAGGCTAGCTCAGTCTTCTTCGCTGCCA CTTCCTGAG
shNC	Forward	CCGGTTCTCCGAACGTGTCACGTTTCAAGAGAACGTGA CACGTTCGGAGAATTTTTG
	Reverse	AATTCAAAAATTCTCCGAACGTGTCACGTTCTCTTGAAA CGTGACACGTTCGGAGAA

Abbreviation: sh, short hairpin; oe, over expression.

Table S2. Primer sequence for RT-PCR

Name		Primer sequence (5' to 3')
DDOST	Forward	ATGGGGTACTTCCGGTGTG
	Reverse	GAAAAGCGAATGAGTCTCCCG
SMARCA4	Forward	ATTGAGAATGCCAAGCAAGATG
	Reverse	ACACCAGCCACTCCAAACCT
GAPDH	Forward	TGACTTCAACAGCGACACCCA
	Reverse	CACCCTGTTGCTGTAGCCAAA

Table S3. Correlation between the mRNA expression level of DDOST and pathological grade in cervical cancer patients from TCGA and our hospital

Data Source	Spearman's rho	*P* value
TCGA	0.162	0.007
Our hospital	0.319	0.022

Table S4. Clinicopathological characteristics of CC patients

Patient Number	Grade	Score	FIGO stage	Histological grade	lymph node metastasis
1	Low	3	II	G1	No
2	High	4	I	G2	No
3	Low	7	I	G1	No
4	Low	4	III	G2	Yes
5	Low	4	I	G1	No
6	Low	2	IV	G3	Yes
7	Low	3	I	G1	No
8	Low	2	II	G1	No
9	High	4	I	G2	No
10	Low	3	I	G1	No
11	Low	4	III	G1	No
12	Low	2	I	G1	No
13	Low	4	II	G3	No
14	Low	4	I	G1	No
15	High	1	I	G2	No
16	Low	2	I	G1	No
17	Low	6	I	G1	No
18	High	8	II	G1	No
19	Low	4	I	G1	No
20	Low	4	I	G1	No
21	Low	3	I	G2	No
22	Low	4	II	G1	No
23	Low	4	I	G3	No
24	Low	4	I	G1	No
25	High	10	I	G2	No
26	Low	4	I	G1	No
27	High	6	II	G1	No
28	High	8	IV	G1	Yes
29	Low	2	I	G3	No
30	High	3	I	G1	No
31	Low	3	I	G1	No
32	High	8	I	G1	No
33	Low	4	I	G2	No
34	Low	2	II	G1	No
35	Low	6	I	G2	No
36	Low	2	I	G1	No
37	Low	3	I	G1	No
38	High	2	III	G1	Yes
39	Low	6	I	G3	No
40	Low	2	I	G1	No
41	Low	8	I	G2	No
42	Low	4	II	G1	No
43	Low	8	I	G1	No
44	High	3	I	G1	No
45	Low	4	II	G2	No
46	High	8	I	G1	No
47	High	4	I	G1	No
48	Low	10	I	G2	No
49	Low	4	II	G1	No
50	Low	4	I	G1	No
51	Low	8	I	G3	No

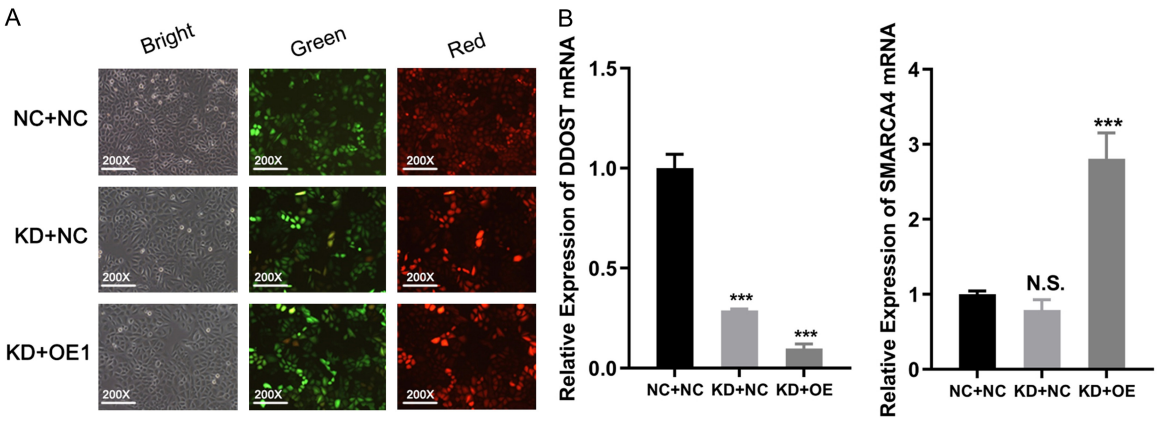

Figure S1. SMARCA4 interacted and exerted synergized role with DDOST in CC cells (A) SiHa cells status 72 h after infection with different lentivirus particles including green fluorescent protein (GFP) or Cherry fluorescence (magnification 200×). NC, control; KD, DDOST knockdown; OE, SMARCA4 overexpression. (B) DDOST knockdown (left) and SMARCA4 (right) overexpression efficiency after co-transfected with lentivirus particles in the presence of puromycin (3 μg/mL). NC, control; KD, DDOST knockdown; OE, SMARCA4 overexpression. Data are presented as mean ± SD from three independent experiments. Statistical significance is indicated as follows: *P < 0.05, **P < 0.01, ***P < 0.001; ns, not significant.

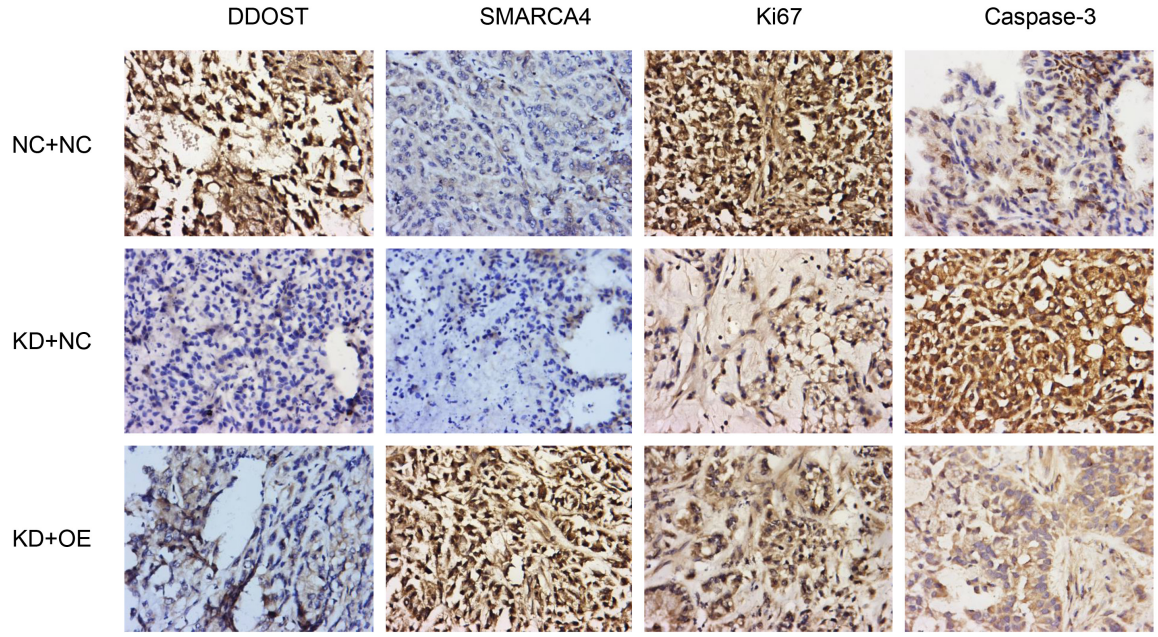

Figure S2. Immunohistochemistry analysis of the tumors was performed to detect the expression of DDOST, SMARCA4, and downstream proliferation markers (Ki-67) and apoptosis markers (cleaved caspase-3).